Journal of Applied Mechanics and Technical Physics, Vol. 40, No. 4, 1999

SPECIAL FEATURES OF SELF-SUSTAINED OSCILLATIONS IN A SUPERSONIC UNDEREXPANDED JET IMPINGING ON AN OBSTACLE WITH A RESTRICTED CROSS-SECTION

G. F. Gorshkov and V. N. Uskov

UDC 533.6.011.5

Effect of the obstacle size on the flow structure and the transient conditions arising in a supersonic underexpanded jet normally impinging on a flat restricted obstacle is studied.

The joint influence of geometric and gas-dynamic parameters on the flow structure and the characteristics of self-sustained oscillations that arise during interaction of a supersonic jet with a normally installed flat obstacle, either infinite or restricted, is governed by the generalized similarity parameter $x_* = 2\mathrm{M}_a(\gamma n)^{0.5}$. In the system "jet–obstacle," steady and unsteady flow regimes alternates as the ratio $h/x_* = H$ varies, where h is the nozzle exit-to-obstacle distance (from here on, all linear dimensions are assumed to be normalized by the nozzle exit-section radius r_a). It is generally believed that the geometric parameter (i.e., the obstacle radius r_p) has a profound effect on the domain of existence of the self-sustained oscillations. However, the latest interesting data on the emergence of the so-called "silence zones" [1] (termination of the oscillations for certain proportions between the obstacle radius r_p and the distance h for supersonic jets with the nozzle pressure ratios $n = 3$ and 5 and Mach numbers $\mathrm{M}_a = 1.5$ and 2) offer a different explanation of the jet interaction phenomenon. In this connection, in this paper, further developing the concept proposed by Glaznev and Popov [1], we study the salient features of the flow and the effect of the obstacle size on the unsteady regimes of the flow around a flat restricted obstacle in a wide range of its radius.

The experimental studies were conducted in a supersonic wind tunnel with a tank air-supply system (stagnation temperature $T_0 = 290$ K). The setup was equipped with a traversing gear, which enabled the obstacle, a cylinder with a flat end, to travel along the jet axis. The covered distance was determined using an electric path marker. Supersonic jets were formed by a conical Laval nozzle installed in a receiver. The Laval nozzle had geometric Mach number $\mathrm{M}_a = 1.5$, semi-vertex angle 5°, and exit-section radius $r_a = 5$ mm.

The pressure fluctuations $p(\tau)$ on the obstacle were measured using a piezoelectric pressure transducer LKh-611 (transmission band of $10–5 \cdot 10^4$ Hz). The instantaneous value of the fluctuations measured by the transducer and amplified by the microphone amplifier 00011 of a 01021 noise-meter manufactured by the RFT firm (transmission band 200 kHz) was recorded by an HO 67 magnetograph (frequency band 40 kHz). In the experiment, the integral level of pressure fluctuations (at the output of the 02022 indicator unit) $\Delta L^0 = 20\log(\sigma/p_w) - L_n$ was also determined, where σ is the effective value of $p(\tau)$, $p_w = 2 \cdot 10^{-5}$ Pa is the hearing-threshold sound pressure, and L_n is the broad-range noise level. The frequency range of the dynamic section "transducer–noise-meter–magnetograph" was wider than 40 kHz for the flatness of the amplitude–frequency response ±3 dB in the above-indicated frequency band. The qualitative pattern of the underexpanded jet flow around the obstacle was monitored using an IAB-45 schlieren device with subsequent photographing.

Baltic State Technical University, St. Petersburg 198005. Translated from Prikladnaya Mekhanika i Tekhnicheskaya Fizika, Vol. 40, No. 4, pp. 143–149, July–August, 1999. Original article submitted September 9, 1997; revision submitted January 26, 1998.

 0021-8944/99/4004-0678 $22.00

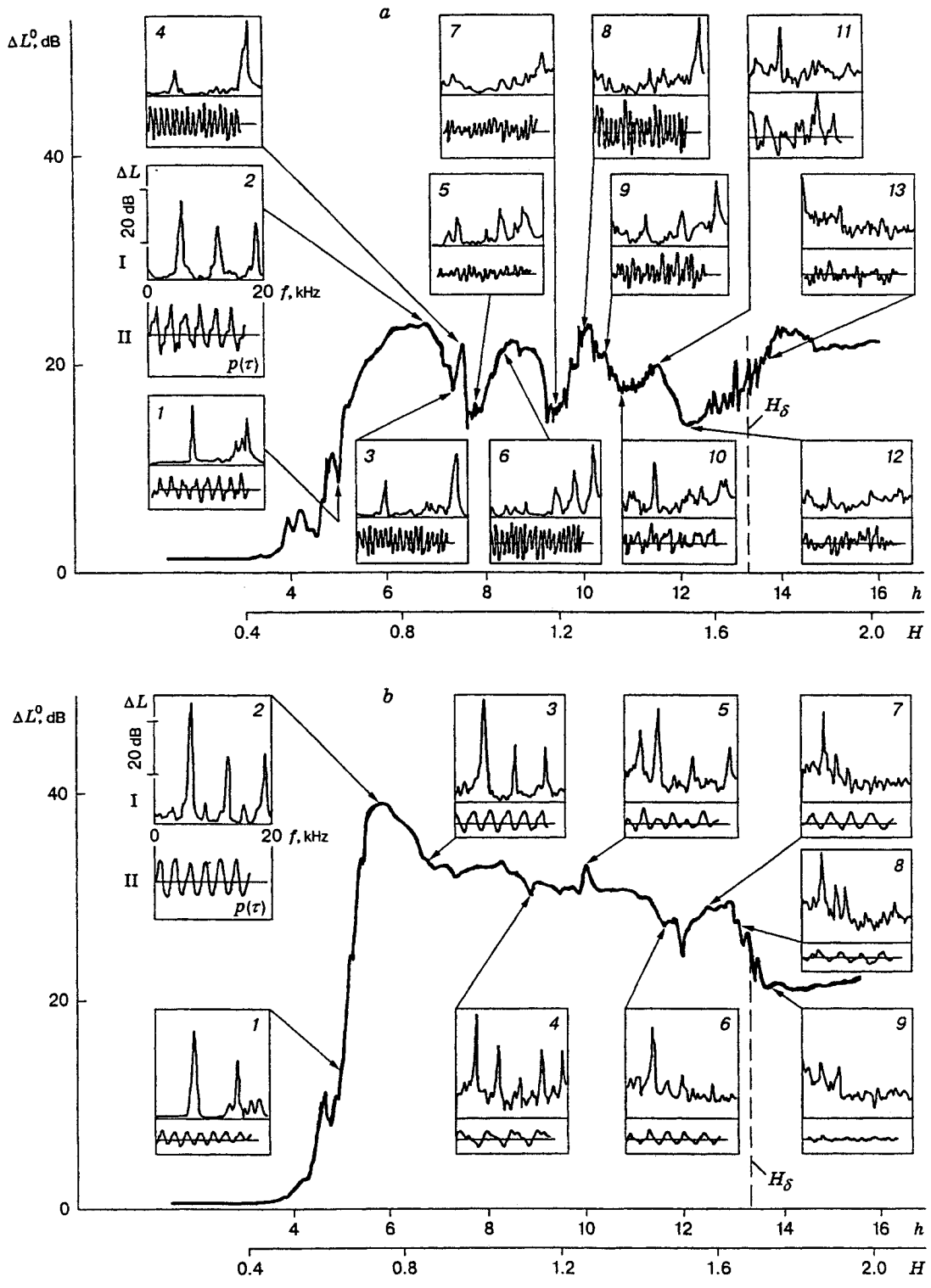
a
ΔL^0, dB
40
20
0
ΔL
20 dB
I
0
20 f, kHz
II
p(τ)
1
2
3
4
5
6
7
8
9
10
11
12
13
H_δ
4
6
8
10
12
14
16 h
0.4
0.8
1.2
1.6
2.0 H
b
ΔL^0, dB
40
20
0
ΔL
20 dB
I
0
20 f, kHz
II
p(τ)
1
2
3
4
5
6
7
8
9
H_δ
4
6
8
10
12
14
16 h
0.4
0.8
1.2
1.6
2.0 H

Fig. 1

The experimental procedure was as follows. For gas parameters at the nozzle exit kept constant, the obstacle slowly moved away from the nozzle along the jet axis (the signal from the transducer was continuously recorded) and the obstacle radius was varied. In the second part of the experiment, the jet impinged on the obstacle at a fixed distance h (h = 5 and 7 for nozzle pressure ratios n = 3 and 5, respectively; steady blowing). The obstacle radius was also varied, the signal being recorded during the blowing. To analyze the amplitude–frequency characteristic of the self-sustained oscillations, we used a set of experimental appliances and a data-processing procedure similar to those described in [2]. The studies were carried out in the following ranges of the parameters: γ = 1.4, M_a = 1.5, n = 3 and 5, r_p = 2.5, 2.8, 3.45, 3.8, 4.6, 5.28, 5.72, 6.27, 6.9, and 7.45, and h = 3–16.

The following experimental results were obtained. In the study, the sequence of flow regimes [2–4] previously established for an obstacle continuously moving away from the nozzle exit was confirmed, together with the emergence of "silence zones" for the oscillations [1]. Some new salient features, which had not been reported previously in the literature (in particular, in [3, 4]), were established. Let us dwell now on these features in more detail.

The succession of the regimes is shown in Fig. 1 by curves of the varied integral level of pressure fluctuations on the obstacle ΔL^0 as functions of the distance h and H for n = 5 [r_p = 5.28 (Fig. 1a) and 2.8 (Fig. 1b)]. For a set of points of these curves marked by arrows, as separate fragments, the following characteristics are shown: the spectra of pressure oscillations (the dependence of the relative level ΔL on the frequency f) (I) and the waveform of pressure oscillations $p(\tau)$ (pressure variation with time) (II).

Points 1 and 2 (Fig. 1a) correspond to the first auto-oscillatory regime (AOR). In the frequency spectra corresponding to these points, multiple discrete components appear, and the pressure oscillations exhibit a clearly pronounced periodic structure. Points 3–9 represent the flow with a central circulation zone. In the frequency spectra for these points, there are no multiple discrete components (except for the high-frequency region), and the pressure oscillations are strongly modulated. In the frequency spectra for points 10–12, a single discrete component appears. The oscillations $p(\tau)$ are also periodic. These points correspond to the second unsteady interaction regime. There are no discrete components in the frequency spectrum (point 13), and the oscillations $p(\tau)$ are random. Point 13 corresponds to an interaction region with an undisturbed first barrel. The distance H_δ (dashed curves), which corresponds to these regimes, is given quite accurately by the dependence derived in [5].

In the experiment, we obtained the curves for the integral level of pressure fluctuations on the obstacle ΔL^0 as a function of H with varied obstacle radius r_p for the jet with n = 3 (Fig. 2a) and n = 5 (Fig. 2b); curves 1–9 correspond to the obstacles with r_p = 2.5, 2.8, 3.45, 3.8, 4.6, 5.28, 5.72, 6.27, and 7.45, respectively. A gradual increase in h always results in an abrupt steady-flow decay: in the system "jet–obstacle," self-sustained oscillations arise and they are accompanied by a substantial increase in the integral level of ΔL^0. The second unsteady regime (points 10 and 11 in Fig. 1a) occurs already at a high level of ΔL^0 and proceeds in a rather sluggish manner compared to the first regime.

Moreover, the analysis of the data obtained shows that, for constant nozzle-exit parameters γ, M_a, and n, there exists a distance h (solid vertical line in Fig. 2) such that self-sustained oscillations do not arise (the first "silence zone" in [1]). For instance, for n = 3, this distance is h = 5 (H = 0.81) (curves 2 and 3 in Fig. 2a). For curve 2, the position of an obstacle of radius r_p = 2.8 corresponds to the emergence of oscillations, whereas for curve 3 the same point for an obstacle with r_p = 3.45 corresponds to their termination. Similarly, for n = 5 and h = 7 (H = 0.88) (curve 5 in Fig. 2b) and r_p = 4.6, the position of the obstacle corresponds to termination of the AOR. In this case, the quantity $R_p = r_p/n^{0.5}$ = 1.6–2.06 agrees with the data [1].

However, every displacement of the obstacle from the above-indicated values of h (both to the left and to the right) for identical obstacle radius r_p again gives rise to self-sustained oscillations, i.e., for fixed M_a, γ, n, and r_p, the "silence zone" arises only for one value of the above-indicated distance h. Thus, the obstacle size does shift the oscillations observed to the boundary of their domain of existence.

The second "silence zone" at R_p = 3–3.5 was not found. This is confirmed by the data of Fig. 2 and the analysis of the relative spectral power of the oscillations of the pressure P^0 at the stagnation point at the frequency of the fundamental tone as a function of R_p, which was constructed using the experimental

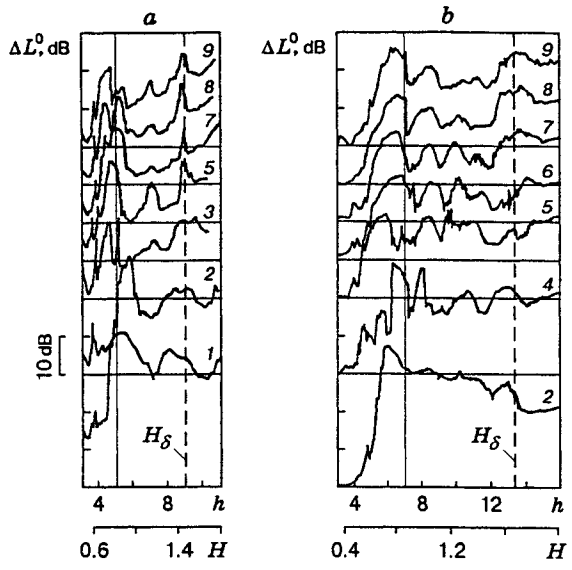

Fig. 2

power–frequency spectra. For the above-indicated range of the parameters, only a local minimum in the P^0 distribution was found.

Using the dependences $\Delta L^0 = f(H)$, we determined the existence limits of unsteady flow regimes on the plane $\{H_{ie,it,\delta};\ R_p\}$, where H_{ie} and H_{it} are the distances, which correspond to the emergence and termination of the unsteady regimes, respectively (Fig. 3). We note that the emergence (decay) of the unsteady regimes was registered by observing the appearance (vanishing) of discrete components in the oscillation spectra (see Fig. 1). For $R_p \geqslant 2$, the obstacle size was found to have practically no effect on the position of the components, i.e., the case $R_p \simeq 2$ is a limiting one.

The analysis of the amplitude–frequency characteristics of pressure fluctuations at the stagnation point of the obstacle [Fig. 3: $r_p = 3.45$ (a) and $r_p = 7.45$ for $n = 5$ (b), the solid curves show the integral level of ΔL^0, the full circles correspond to the frequencies of the fundamental tone f_r, the dashed vertical lines separate the emergence and termination of the unsteady regimes, the dot-and-dashed line corresponds to a radial flow with an undisturbed first jet barrel H_δ, the first and the second regimes are indicated by I and II, respectively], together with the analysis of the boundaries of existence of the unsteady regimes, allowed the following two types of obstacles with certain characteristic sizes to be established:

— "small obstacles" ($R_p < 2$), for which both unsteady regimes are observed (Fig. 3a); they occupy the entire range of H up to the appearance of a flow with an undisturbed first barrel (dot-and-dashed line H_δ);

— "large obstacles," for which two unsteady regimes separated by the flow region with the central circulation zone (Fig. 3b) are also observed.

For the "small obstacles," the transition from the first to the second region occurs abruptly (as evident from the data of [6] for rarefied jets interacting with a normally installed flat restricted obstacle). In the literature, it was believed [3, 4] that only one AOR existed in the case of dense jets (within the range of distances $h \leqslant H_\delta$). In addition, obstacles with the generalized parameter $\mathrm{M}_a/r_p^2 > 0.1$ were understood as "small obstacles" in [4] (the domain of AOR existence in this case is closed). From here, for $\mathrm{M}_a = 1.5$ and $n = 3$ and 5, we obtain $R_p < 15/n^{0.5} = 2.23$–$1.73 \simeq 1.98$ (the mean value), which is just the case for our experiment. For "small obstacles," the domains of existence of two regimes plotted in the generalized coordinates $\{h/(r_p \mathrm{M}_a^{0.5}),\ (n\mathrm{M}_a^{0.5}/r_p^2)\}$ merge together forming a single domain.

It seems that the reason for no reported observations of the second regime at earlier stages of the AOR studies (e.g., in [3]) can be explained by numerous shortcomings of the test procedures and experimental facilities used.

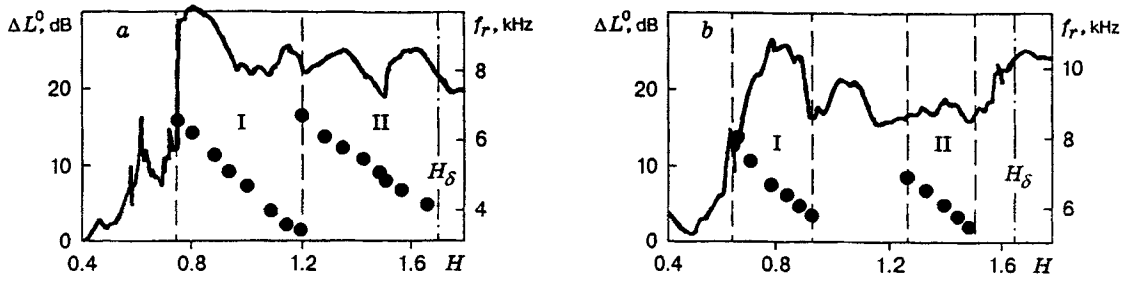

Fig. 3

For the indicated types of obstacles, the first regime of self-sustained oscillations is characterized by the presence of several discrete components in its frequency spectrum (in addition to the fundamental tone, harmonics up to 40 dB are distinctly observed, which is higher than the overall level of the jet noise) (see curves I, which correspond to points 1 and 2 in Fig. 1a and to points 1–5 in Figs. 1b, respectively). The first AOR exhibits strong oscillations of the shock-wave structure and the pressure on the obstacle, which have a large amplitude and comparatively low frequency. The oscillations in this case have a clearly pronounced periodic structure.

The second regime, far less extended (2–5 times narrower than the first regime), is characterized by the presence of a single discrete component (about 40–30 dB) in its frequency spectrum (curves I, which correspond to points 10 and 11 in Fig. 1a and points 6–8 in Fig. 1b) and moderate oscillations of the shock-wave structure and pressure on the obstacle (curves II).

For the unsteady regime of the flow around the obstacle, the increase in the distance results in a monotonic decrease in the fundamental frequency, whereas upon transition from the first to the second regime, it increases only slightly (see Fig. 3). However, only for "small obstacles" does this increase "recover" the frequency f_r to the values typical for the emergence of self-sustained oscillations (Fig. 3a).

The analysis of the frequencies of the unsteady processes showed that there is only one discrete component in the frequency spectra on the segments where the oscillations arise and decay (see, e.g., the curves that correspond to points 1 and 3 in Fig. 1a), which rises to a rather high level (15–25 dB) above the underlying wide-range background. The presence of several (multiple) discrete components in the frequency spectrum results from the nonlinearity of pressure fluctuations caused by the shock-wave processes proceeding in the region between the central compression shock (CCS) and the obstacle.

The parameters of the system "CCS–obstacle" have an impact on the frequency f_r of pressure fluctuations. An increase in the CCS-to-obstacle distance Δ with increasing H, as well as with increasing n and M_a [2–4] for both regimes, is accompanied by a decrease in the frequency f_r. On this basis, introducing the complex $d_a n^{0.5}$, where $d_a = 2r_a$, as a cross-sectional dimension of the shock layer, one can generalize the frequency characteristics of both processes (to an accuracy within 10%) by the universal empirical dependence

$$\mathrm{Sh}_r^{-1} = a_0/(f_r d_a n^{0.5}) = A_i \Delta/(d_a n^{0.5}) + B_i,$$

where $A_1 = 4.1$ and $B_1 = 0.6$ (the first regime), $A_2 = 1.8$ and $B_2 = 0.4$ (the second regime), a_0 is the speed of sound in the stationary gas, and Δ is the distance from the obstacle around which the CCS vibrates (the mean value of Δ is borrowed from [4]).

The second part of the studies of jet flows around obstacles was conducted for a fixed distance h ($h = 5$ and 7 for $n = 3$ and 5, respectively). In this case, the obstacle radius was varied. Here, we dwell on these results in more detail. As noted above, only the occurrence of the first "silence zone" has been experimentally confirmed ($R_p \simeq 2$).

The effect of the obstacle radius on the frequency characteristics of the unsteady regimes for "small obstacles" manifests itself in a lower Strouhal number ($\mathrm{Sh}_r = 0.365 = \mathrm{const}$) compared to the case of "large obstacles" ($\mathrm{Sh}_r = 0.4 = \mathrm{const}$). The value of the dimensionless parameter $R_p \simeq 2$ is also a limiting one.

The phenomena that accompany the emergence and termination of an unsteady regime are important

specific features of the jet interaction under study. In the case under consideration, such features are exhibited by the flow at distance h to the left and to the right from the "silence zone." For instance, for a fixed value of the generalized parameter H, it has been established that, in spite of the presence of a discrete component in the averaged spectrum of pressure fluctuations (~15 dB), the instantaneous gas oscillations exhibit a relaxation behavior. The latter is manifested as follows:

(1) The amplitude of pressure oscillations changes considerably in time (its minimum value is close to zero and the maximum value is equal to the amplitude of fully developed self-sustained oscillations, i.e., the amplitude is modulated);

(2) The frequency of the oscillations changes from a relatively low frequency to a high value determined by the jet noise spectrum;

(3) The shock-wave structure ahead of the obstacle observed with the IAB-451 device (the exposure time of the camera was far longer that the period of oscillations) is stationary and a sequence of standing waves appears between the nozzle and the obstacle (a sequence of alternating light and dark strips radially diverging from the obstacle).

Finally, we outline some peculiar features of gas spreading over the obstacle surface and make several assumptions about the emergence of "silence zones" for certain obstacle sizes. Glaznev and Popov [1], within the framework of some model considerations of self-sustained oscillations, offered an explanation for this anomalous phenomenon. However, the fact that the numerical values of r_p, for which these zones exist, coincide with (are close to) the numerical values of the coordinates r, for which discontinuities in the distributions of the acoustic potential $\varphi(r)$ are observed, is not a physical reason for the termination of the oscillations.

In our opinion, this phenomenon can be explained by some specific features of gas spreading over the surface of a flat obstacle. For example, an analysis of the gas flow past it, which was performed using the schlieren pictures of the shock-wave structures, showed that, for an identical value of H, a restricted flat obstacle deflects the flow differently after this flow is accelerated from the stagnation point. The following features can arise upon the gas deflection by a sharp edge of the obstacle, depending on the obstacle radius r_p:

— a fan jet deflected downstream ("small obstacles");

— a free supersonic radial jet normal to the main-flow axis (as a rule, observed in the case of "small obstacles");

— a near-wall radial supersonic jet (radial gas spreading predominantly along the obstacle, which is observed for "large obstacles").

In addition, in the wall boundary layer, there are concentric zones (filaments) of periodic flow detachment and reattachment, the so-called cellular vortices with an intense reverse gas flow [7, 8]; the boundary layer separation occurs in the subsonic or weakly supersonic flow. The interaction between the near-wall flow and the external (relative to it) stream can result in the above anomaly. However, this hypothesis needs further confirmation.

Thus, the generalized obstacle radius R_p and the dimensionless distance H (similarity parameter h/x_*) are the governing factors of the oscillatory processes [9], and they should be taken into account when designing physical and mathematical models for various auto-oscillatory regimes.

REFERENCES

1. V. N. Glaznev and V. Yu. Popov, "Effect of the flat-obstacle size on self-sustained oscillations that arise in a supersonic underexpanded jet flow around the obstacle," *Izv. Ross. Akad. Nauk, Mekh. Zhidk. Gaza*, No. 6, 164–168 (1992).
2. G. F. Gorshkov, V. N. Uskov, and V. S. Favorskii, "Nonstationary flow of an underexpanded jet flow around an infinite obstacle," *Prikl. Mech. Tekh. Fiz.*, **34**, No. 4, 58–65 (1993).
3. G. V. Naberezhnova and Yu. N. Nesterov, "Unsteady interaction between a diverging supersonic jet and an obstacle," *Tr. TsAGI*, No. 1765 (1976).
4. V. A. Ostapenko and A. V. Solotchin, "Force action of a supersonic underexpanded jet on a flat obstacle," *Izv. Sib. Otd. Akad. SSSR, Ser. Tekh. Nauk*, **13**, No. 3, 26–32 (1974).

5. B. G. Semiletenko and V. N. Uskov, "Experimental dependences determining the location of shock waves in a jet impinging on an obstacle normal to its axis," *Inzh. Fiz. Zh.*, **23**, No. 3, 453–458 (1972).
6. G. F. Gorshkov and V. N. Uskov, "Self-sustained oscillations in supersonic impact jets," in: *Fundamental Research in Aerospace Science*: Book of Abstracts of Int. Conf. (Zhukovskii, Russia, Sept. 22–24, 1994), Sec. 3, TsAGI, Zhukovskii (1994).
7. I. A. Belov, I. P. Ginzburg, V. A. Zazimko, et al., "Effect of jet turbulence on the heat transfer from the jet to an obstacle," in: *Materials of the III All-Union Meeting on Heat and Mass Transfer* (Minsk, 1968), Vol. 11, Inst. of Heat and Mass Transfer, Belarus. Acad. of Sci., Minsk (1969), pp. 167–186.
8. I. A. Belov, I. P. Ginzburg, G. F. Gorshkov, et al., "Urgent topics on heat transfer between a jet and an obstacle," in: *Mater. IV All-Union Meeting on Heat and Mass Transfer* (Minsk, 1972), Vol.1, Part 2, Inst. of Heat and Mass Transfer, Belarus. Acad. of Sci. Minsk (1972), pp. 271–281.
9. G. F. Gorshkov and V. N. Uskov, "Controlling the flow structure and characteristics of supersonic impact jets," in: *Jet and Unsteady Flows in Gasdynamics*: Abstracts XVI All-Russia Seminar, Inst. of Theor. and Appl. Mech., Sib. Div., Russian Acad. of Sci., Novosibirsk (1995), pp. 21–22.